forests

MDPI

Article

Influence of Early-Season Drought on the Peak of Growing Season in China Varies by Drought Timing and Biomes

Zexing Tao, Junhu Dai, Xiaoyue Wang and Yuan Wang *

Institute of Geographic Sciences and Natural Resources Research, Chinese Academy of Sciences, Beijing 100101, China
* Correspondence: wangyuan@igsnrr.ac.cn

Abstract: The peak of growing season (POG) represents the timing of the maximum capacity of vegetation photosynthesis and acts as a crucial phenological indicator for the carbon cycle in terrestrial ecosystems. However, little is known about how POG responds to extreme climate events such as drought across different biomes. Based on two drought indices, we analyzed the temporal–spatial pattern of drought and POG in China and then investigated how drought influenced the POG in different periods of the early season through correlation analysis. In general, a trend towards increased aridity and earlier POG was found in most areas. The impact of drought on POG differed among periods. On the one hand, an earlier POG enabled plants to reduce evapotranspiration and mitigate the risk of severe summer drought. On the other hand, the drought that occurred in spring impeded plant growth and caused a delay in spring phenology, thereby postponing POG. Summer drought led to an earlier POG in relatively dry biomes but inversely led to a later peak in photosynthetic activity in wetter biomes. We also observed a 1-month/2-month lagged effect of drought on POG in almost half of the areas and a 2-month/ 3-month cumulative effect of drought in the north of 50° N. These findings enhance our understanding of carbon uptake in terrestrial ecosystems by clarifying the mechanisms by which climate change impacts vegetation growth and photosynthetic activity.

Keywords: drought index; standardized precipitation-evapotranspiration index; peak of growing season; correlation analysis; China

Citation: Tao, Z.; Dai, J.; Wang, X.; Wang, Y. Influence of Early-Season Drought on the Peak of Growing Season in China Varies by Drought Timing and Biomes. *Forests* **2024**, *15*, 1027. https://doi.org/10.3390/f15061027

Academic Editor: Romà Ogaya

Received: 8 May 2024
Revised: 7 June 2024
Accepted: 11 June 2024
Published: 13 June 2024

1. Introduction

Plant phenology is one of the most sensitive ecological indicators of climate change [1–4]. The seasonal dynamics of phenology have a major impact on the carbon cycle, the water cycle, and the exchange of land–air energy in the ecosystem [5–9]. The spring and autumn phenophases, such as the beginning of the growing season and the end of the growing season, have been thoroughly investigated regionally or globally over the past few decades based on remote sensing data [10–12]. In comparison, another important phenological metric in summer—the peak of growing season (POG)—has been given less attention. POG is usually derived from the time series of vegetation index (VI) and is identified as the time when the smoothed VI curve reaches the maximum [13,14]. Many studies have suggested that POG is an important indicator of terrestrial gross primary production (GPP) variability as it can indicate the timing of the maximum capacity of photosynthesis, i.e., the maximum capacity of CO_2 uptake [15–17]. In addition, POG is intimately related to the timing of maximum plant resource availability. Changes in POG can affect the habitat of upper trophic-level predators. For example, an earlier onset of POG in the temperate grasslands of China was associated with increasing annual production, thereby providing more forage for livestock [18]. The timing of POG also significantly influenced surface albedo and energy balance [14,19,20].

Previous studies have suggested a trend towards an earlier POG for most mid-latitude vegetation in the Northern Hemisphere from 1982 to 2012, with significant trends averaging

0.61 day/a in 19.4% of the areas [21]. In comparison, Gonsamo et al. [14] found a relatively weaker advancing trend of 0.12 day/a in POG across extratropical terrestrial ecosystems in the Northern Hemisphere from 1982 to 2015. In China, a trend of 0.14 day/a towards an earlier POG was observed in 67.2% of the regions during the same period [19]. These results indicated that the temporal changes in POG were divergent with respect to different regions and biomes, which needed to be investigated comprehensively, particularly for those at low latitudes.

The shifts in POG reflect the response and adaptive strategy of vegetation to environmental change. On the one hand, warmer spring temperatures may lead to a more rapid accumulation of heat and, consequently, an earlier start of the growing season [22,23], thus allowing vegetation to reach its maximum growth earlier. On the other hand, a shift towards early POG enables vegetation to benefit from mild temperatures and high soil moisture in spring [21,24] and to avoid potential damage in unfavorable high summer temperatures and drought [14,25]. In arid and semi-arid regions, where low temperatures are not a key issue, the advance in POG has been widely attributed to a reduction in water resources [21]. For example, Wang and Wu [19] found significant correlations between POG and preseason precipitation in almost 30% of the areas in China, with negative correlations mainly distributed in southeast China, the southwest Tibetan Plateau, and north Inner Mongolia [19]. Studies also suggested that droughts alter phenological sensitivity and synergistically lower ecosystem production [26]. Thus, it is necessary to identify the plant physiological mechanisms underlying how POG changes under arid conditions in order to obtain reliable predictions of ecosystem productivity [24–28].

Over the past several decades, climate change has precipitated a global increase in tree mortality and forest die-offs because of hotter droughts [27]. In the Northern Hemisphere, drought has been recognized as one of the most detrimental natural disasters in many regions [28,29], including the western United States, southeastern Australia, and Russia [30,31]. Regarding China, drought events have escalated in severity and frequency in the southwest and parts of the eastern northwest from 1965 to 2017 [32], with the potential for further expansion under future climate change scenarios [28,33]. As a result, the objectives of this study are to (1) analyze the temporal–spatial patterns in the peak of growing season and drought events based on two drought indices across different biomes in China and (2) to investigate how drought influenced POG in different preseason periods using correlation analysis. We hypothesize that the regional difference in drought events will lead to a phenological pattern characterized by significant spatial disparities. In addition, the response of summer phenology to drought depends on the timing of drought events.

2. Data and Methods

2.1. Study Area

China has complex terrain and diverse vegetation types (Figure 1). In total, 14 biomes were identified according to a digitized 1:1,000,000 vegetation map of China that was obtained from the National Earth System Science Data Sharing Infrastructure, National Science & Technology Infrastructure of China (http://www.geodata.cn, accessed on 11 April 2021). Within the region, temperature evidently decreases from north to south, and precipitation decreases from east to west (Figure 1c,d).

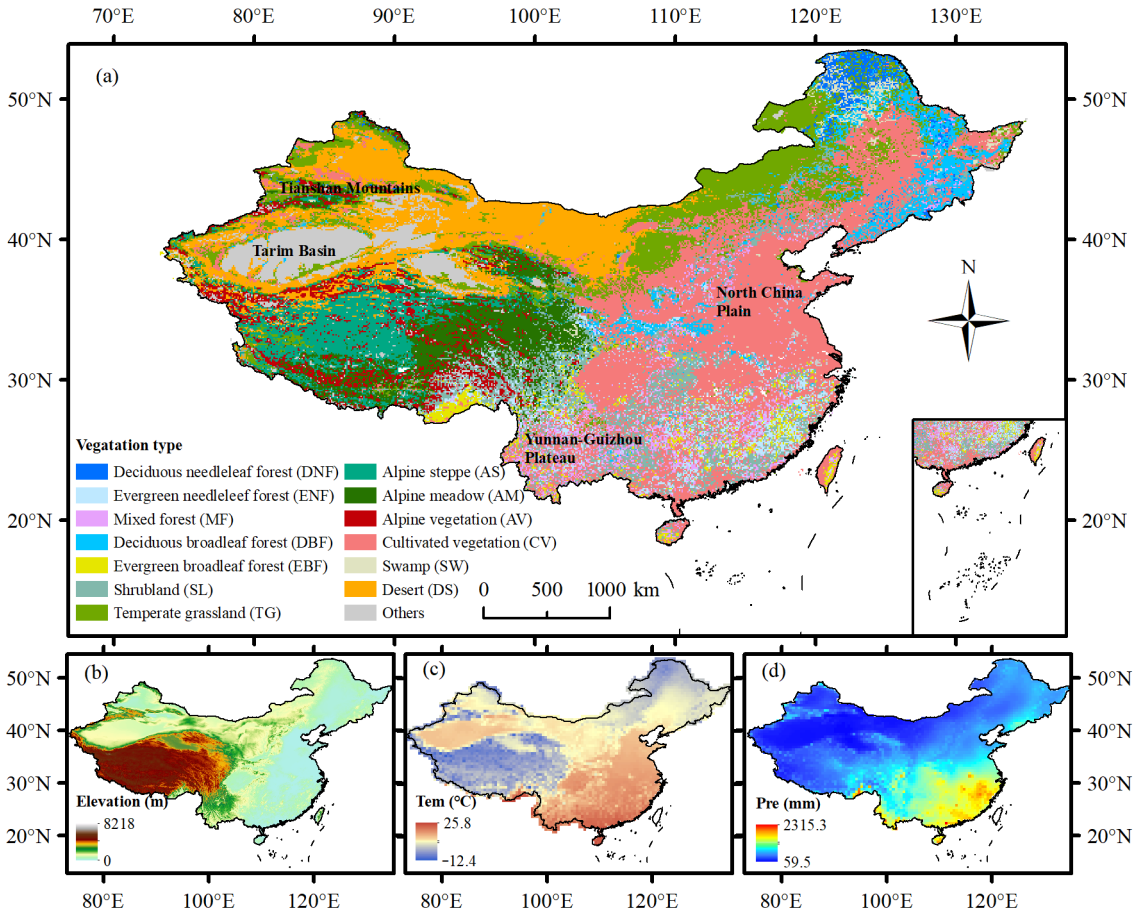

Figure 1. Vegetation type (**a**), elevation (**b**), annual mean temperature (**c**), and annual total precipitation (**d**) of the study area. The locations of some less-known regions mentioned in the text are shown.

2.2. Data Sources

2.2.1. Normalized Difference Vegetation Index Data

The Normalized Difference Vegetation Index (NDVI) data with a spatial resolution of 1/12° and a temporal resolution of 15 days from 1982 to 2015 were derived from the GIMMS3g. v1 dataset (https://data.tpdc.ac.cn/en/data/9775f2b4-7370-4e5e-a537-3482c9a83d88/, accessed on 10 May 2022) [34]. The NDVI pixels with an annual mean value below 0.15 were removed to reduce the noise from the soil background or other surfaces with sparse vegetation [35].

2.2.2. Meteorological Data

The monthly meteorological data, including mean air temperature (Tem), precipitation (Pre), surface downward shortwave radiation (Srad), and wind speed (Wind) from 1980 to 2015 were obtained from the China Meteorological Forcing Dataset, which has a spatial resolution of 0.1° [36]. The dataset has been well-validated and widely used in previous studies [37].

2.2.3. Drought Data

We quantified drought conditions from 1980 to 2015 in terms of the water balance ratio by two datasets. Firstly, the 0.5° gridded monthly precipitation and potential evapotranspiration (ET_0) was obtained from the Climate Research Unit (CRU) dataset (TS v4.03), and the drought index (DI) was computed as Pre/ET_0 for each month [29]. Then, the Standardized Precipitation-Evapotranspiration Index (SPEI) from the SPEIbase v2.5 dataset

(https://digital.csic.es/handle/10261/153475, accessed on 12 July 2011) was used for comparison, which also has a spatial resolution of 0.5° [38]. The SPEI is a multiscalar index expressing the deviations in the current climatic balance with respect to the long-term balance, and the SPEI at 1-, 2-, and 3-month time scales (i.e., 1-month SPEI, 2-month SPEI, and 3-month SPEI) was used for analysis in this study. Smaller values of DI/SPEI indicate a higher degree of drought.

2.3. Methods

2.3.1. Extraction of POG

We used a modified Savitzky–Golay filter to smooth the raw NDVI series, with a smoothing window of 4 and iteration time of 20, so that the NDVI series was interpolated to a daily time scale between the GIMMS observations (Figure 2). Subsequently, a negative exponential model based on polynomial regression and weights computed from the Gaussian density function was applied to the smoothed NDVI curve. The maximum NDVI in summer ($NDVI_{max}$) was then calculated, and the date on which the $NDVI_{max}$ occurred was defined as POG (DOY).

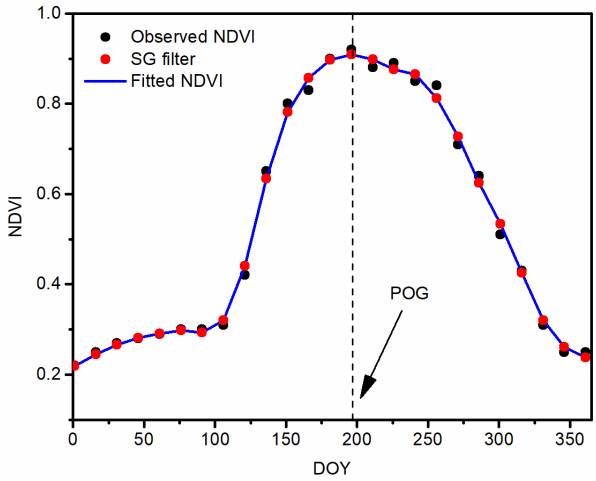

Figure 2. Schematic for the peak of growing season (POG) derived from the NDVI curve.

We also obtained land cover data every 5 years from 1980 to 2015 from the Data Centre for Resources and Environmental Sciences (RESDC) of the Chinese Academy of Sciences [39]. The pixels with dramatic changes in land cover types during this period (e.g., from forest to grassland) were removed from further analysis [35].

2.3.2. Trends and Correlation Analysis

The Theil–Sen estimator was employed to calculate the trends in both the drought index and POG, which is notably insensitive to outliers [40]. The Mann–Kendall function was utilized to determine significance at a 0.05 level.

To examine the influence of drought on POG, we calculated Pearson's correlation coefficient between POG and DI/SPEI ($R_{POG\_drought\ index}$) for each of five potential influencing periods, i.e., the current month of the multiyear average POG (M0), the 1st month before the multiyear average POG (M1), the 2nd month before the multiyear average POG (M2), the current and 1st month before the multiyear average POG (M0-1) and the current, 1st, and 2nd month before the multiyear average POG (M0-2), because plant phenology is mainly affected by droughts in the preseason 1–3 months [41]. Subsequently, the absolute values of the correlation coefficients were compared. The occurrence of the maximum absolute correlation coefficient (|Rmax|) in M0, M1, M2, M0-1, and M0-2 indicated no lagged or cumulative effect, 1-month lagged effect, 2-month lagged effect, 2 months cumulative effect, or 3-month cumulative effect of DI/SPEI on POG, respectively.

3. Results

3.1. Temporal and Spatial Pattern of Drought Conditions

The DI showed an evident increasing pattern from northwest to southeast China from 1982 to 2015, with a range from 0.01 to 2.8 (Figure 3), indicating a relatively humid environment around southeastern coastal areas. The spatial standard deviation ranged from 0 to 0.54, with an average value of 0.11. The SPEI in northwest China (around the Tarim Basin) and north central China was negative, and the 3-month SPEI was significantly lower than the 1-month and 2-month SPEI. This suggests that drought in this region was more intense on a seasonal time scale. Furthermore, we observed that the standard deviation of the 3-month SPEI was greater than that of the 2-month and 1-month SPEIs, suggesting a higher frequency of fluctuations in SPEI over seasonal time scales.

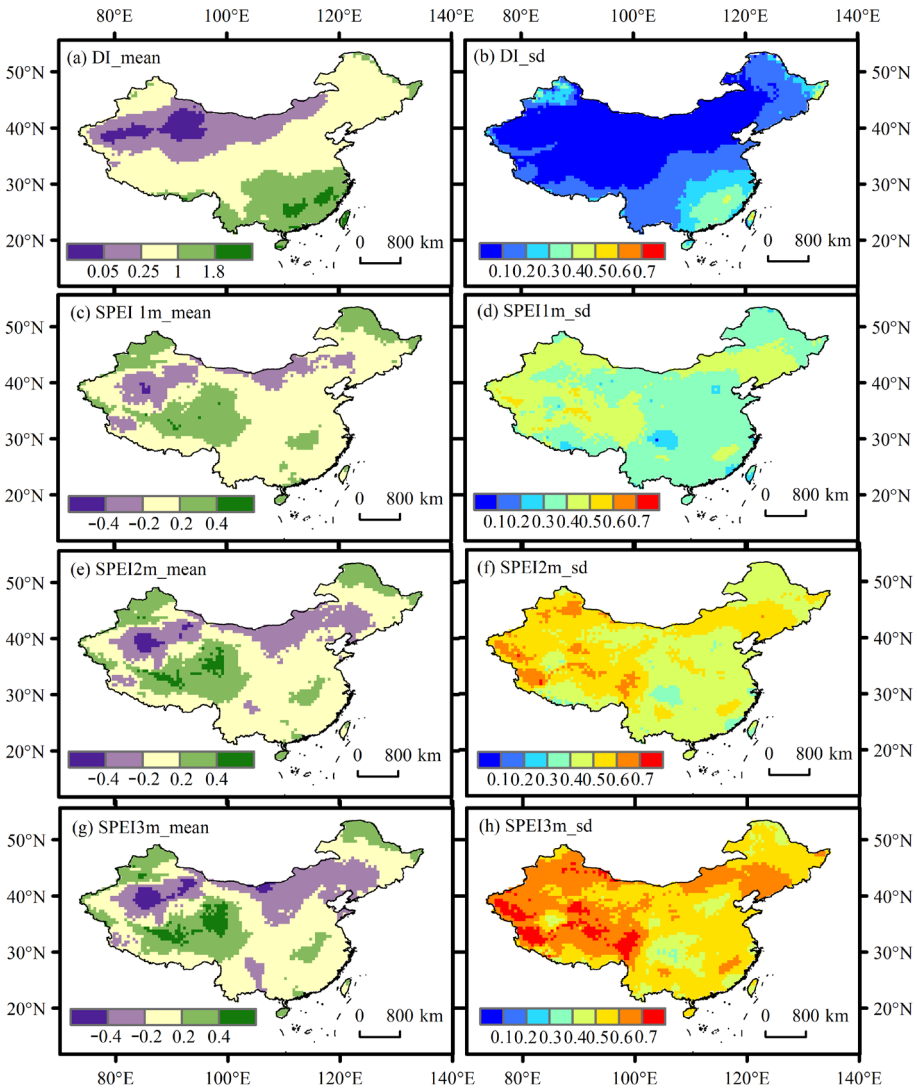

Figure 3. Spatial patterns in the multiyear mean and standard deviation of DI (**a**,**b**), 1-month SPEI (**c**,**d**), 2-month SPEI (**e**,**f**), and 3-month SPEI (**g**,**h**) from 1982 to 2015.

The spatial pattern of the trends in the drought index based on the Theil–Sen slope and MK test are displayed in Figure 4. From 1982 to 2015, the DI decreased in 52.9% of the total area, but the trend was only significant ($p < 0.05$) for 10% of the pixels. The trend in SPEI was almost consistent in terms of different time scales. The pixels with decreased 1-month, 2-month, and 3-month SPEI accounted for 72.2%, 75.0%, and 78.5% of the total area, respectively, indicating a trend towards arid conditions in most areas. The significant

decreasing trends in SPEI were majorly distributed around the Tarim Basin in northwest China and the Yunnan-Guizhou Plateau in the southwest ($p < 0.05$). On the contrary, the SPEI in merely a small portion of northeast China showed a significant increasing trend ($p < 0.05$).

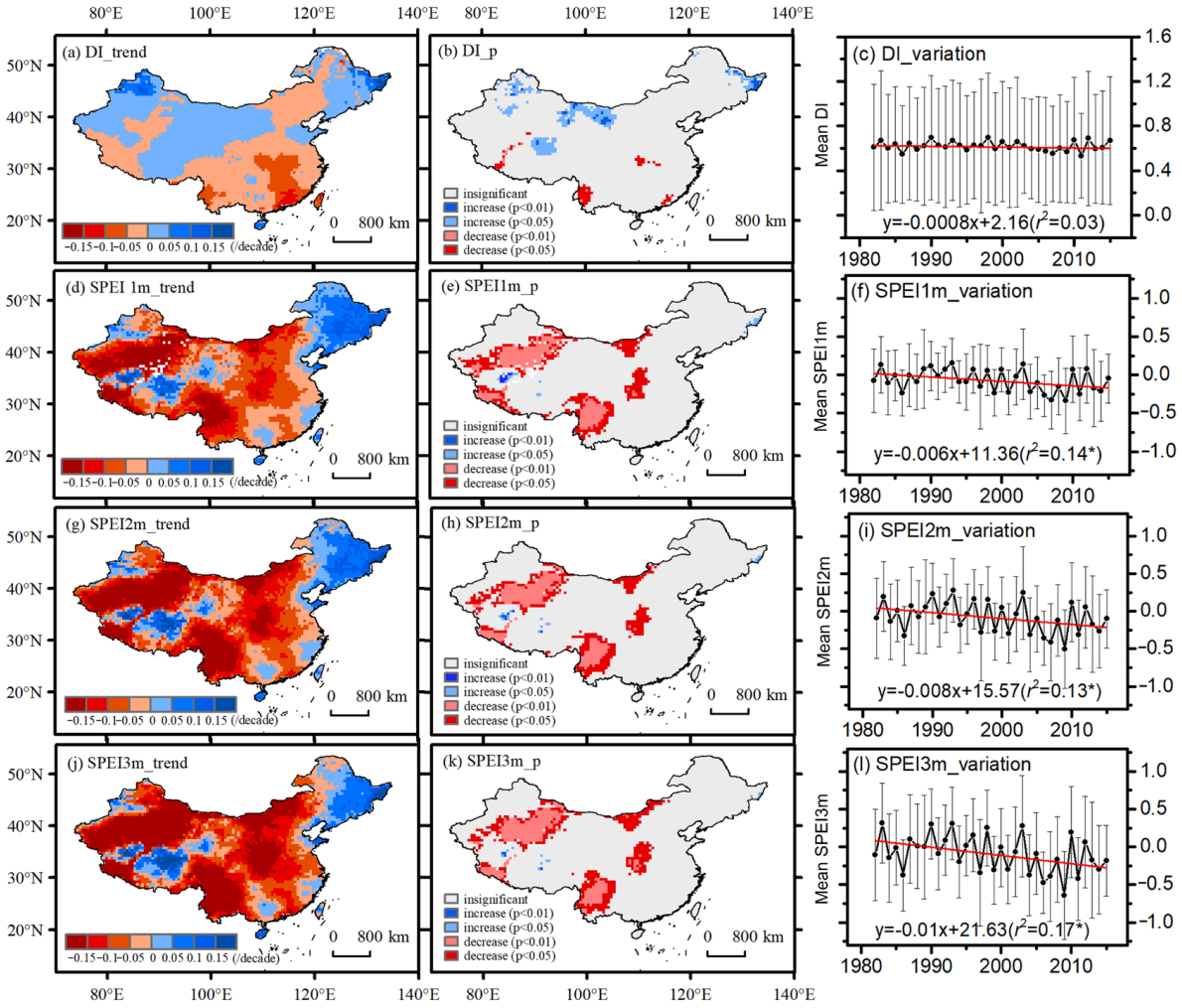

Figure 4. Spatial patterns of the trend, *p*-value, interannual variation in mean DI (**a**–**c**), 1-month SPEI (**d**–**f**), 2-month SPEI (**g**–**i**), and 3-month SPEI (**j**–**l**) from 1982 to 2015. The asterisk indicates $p < 0.05$. The red lines depict the linear fitting trends, while the grey vertical lines signify the standard variation in space.

3.2. Temporal and Spatial Patterns of POG

The mean POG in 73.3% of the pixels ranged from the end of June (DOY: 180) to early August (DOY: 220) from 1982 to 2015 (Figure 5). The earliest POG, occurring around late April, was mainly located in the north of the Tianshan Mountains in the northwest and parts of central China. Conversely, the latest POG, which occurred around October, was predominantly found in the southern border of China. In terms of the interannual difference, the standard deviation of POG in south China exceeded 30 days, while it was less than 10 days in northeast China and the western Tibetan Plateau. It is worth noting that the POG of EBF (mean DOY: 252) was evidently later than that of other biomes, for example, the mean POG of DBF was almost 2 months earlier than EBF. In terms of needleleaf forest, the POG of DNF (mean DOY: 191) was more than one month earlier than ENF (mean DOY: 229).

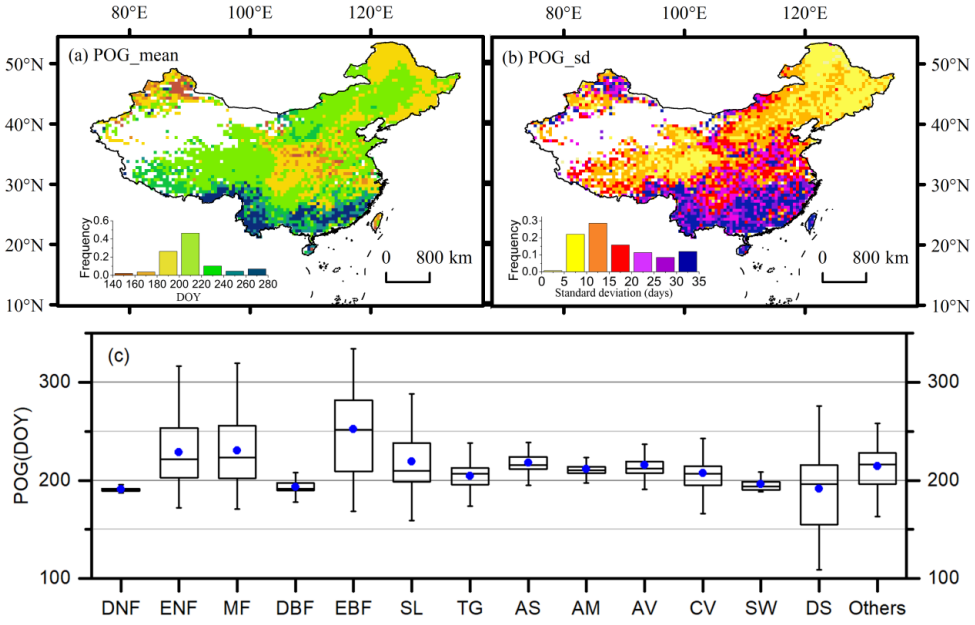

Figure 5. Spatial patterns of the multiyear mean (**a**) and standard deviation (**b**) of the peak of growing season (SOG) and boxplot of POG for different biomes (**c**) from 1982 to 2015. The abbreviations for different biomes correspond to those in Figure 1.

In general, 65.1% of the pixels exhibited a trend towards earlier POG (Figure 6), with a significant advancing trend ($p < 0.05$) distributed around the North China Plain. The significant delaying trend in POG was only distributed in parts of the areas in the northeast and Yunnan-Guizhou Plateau in southwest China. For all biomes except DBF, AS, and SW, a trend towards earlier POG was observed in more than half of the areas, although only 30% of the trends were significant ($p < 0.05$). In particular, the proportion of advancing trends in DNF was comparable to that in ENF, but the spatial difference in these trends was more pronounced in ENF.

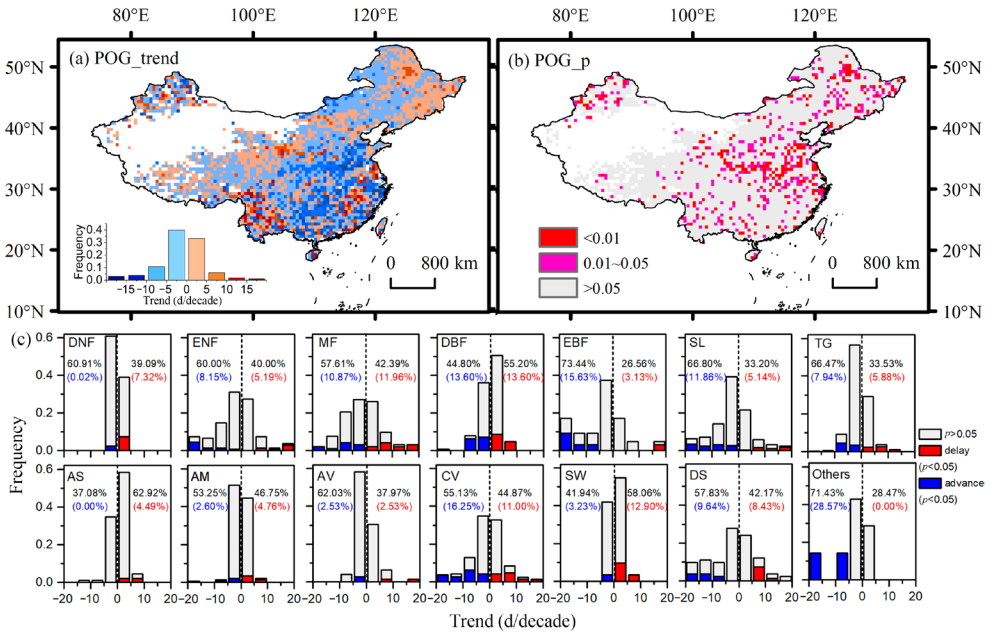

Figure 6. Spatial patterns of the trend (**a**) and *p*-value (**b**) in the peak of growing season (POG) and frequency distribution of the trend in POG for different biomes (**c**) from 1982 to 2015.

3.3. Influence of Drought on POG

Through correlation analysis, we revealed how the preseason drought affected the POG in different periods (Figures 7 and S1). Both the DI and SPEI in the current month of the multiyear average POG (M0) were positively correlated with annual POG in ca. 65.0% of the total areas, indicating that a drought near POG would lead to an early POG in most areas. Negative and significant correlations between current-month DI/SPEI and POG were mainly found in the northeast. However, the DI/SPEI in the first and second month before the multiyear average POG was negatively correlated with POG in ca. 50%~60% of the areas, suggesting that the drought in the preseason 2 months might inversely lead to a later POG in most areas. The areas showing negative correlations were largely located in northern China.

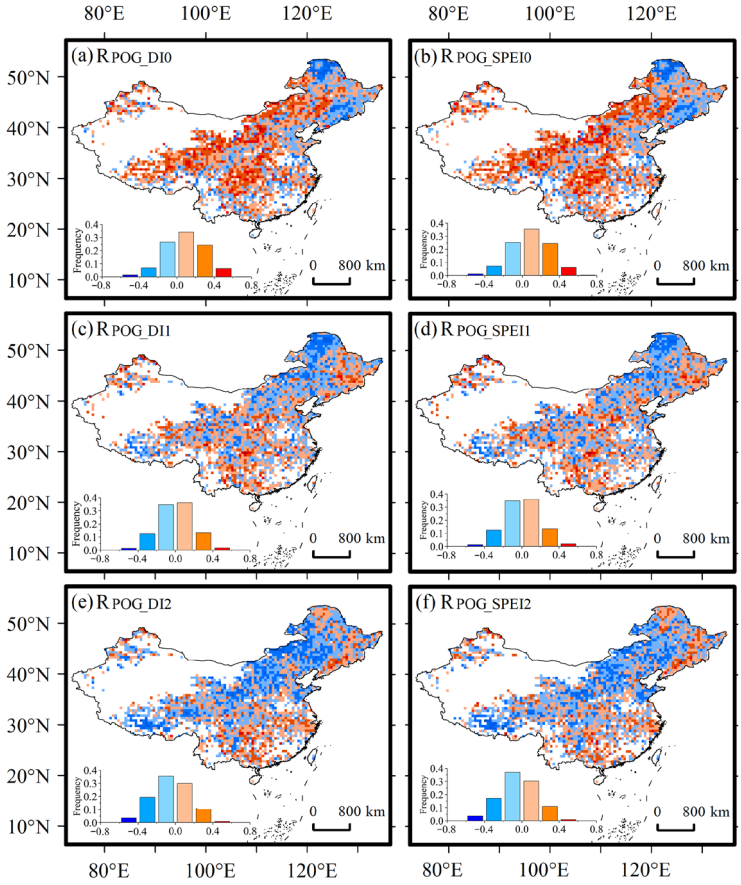

Figure 7. Pearson's correlation coefficients and *p*-values between POG and DI/SPEI in different periods. The numbers 0, 1, and 2 in the subtitles (**a**–**f**) represent the DI/SPEI in the current month of the multiyear average POG (M0), 1st month before the multiyear average POG (M1), 2nd month before the multiyear average POG (M2), respectively.

The lagged effect and cumulative effect of DI/SPEI on POG were shown by the absolute maximum correlation coefficient (Figure 8). Overall, approximately 30% of the areas showed no lagged effect or cumulative effect, about 50% of the areas presented a 1-month or 2-month lagged effect, and about 20% of the areas displayed a cumulative effect of 2 months or 3 months. Notably, the cumulative effect was more pronounced in the area north of 50° N.

The correlations classified by biomes are shown in Figure 9. For all the biomes except DNF, DBF, and SW, the DI/SPEI in M0 was positively correlated with POG in most parts of the areas, suggesting that a relatively wetter condition in the growing season would postpone the POG in most biomes. Regarding DNF and SW, the increase in DI/SPEI in M0 would inversely lead to an earlier POG in 85.0% (significant: 37.5%~40.0%) and 74.2% of

the areas (significant: 9.7%), respectively. In addition, significant correlations were seldom found between the POG and DI/SPEI in M2 for most biomes, which implied that the moisture condition in the early season had weak influences on POG. We also noticed that the DI/SPEI had an evident 2-month accumulative effect on the POG of DNF and SW, with ca. 60.0% and 16.1% of the areas presenting a significantly negative correlation between the POG and DI/SPEI in M0-1, respectively.

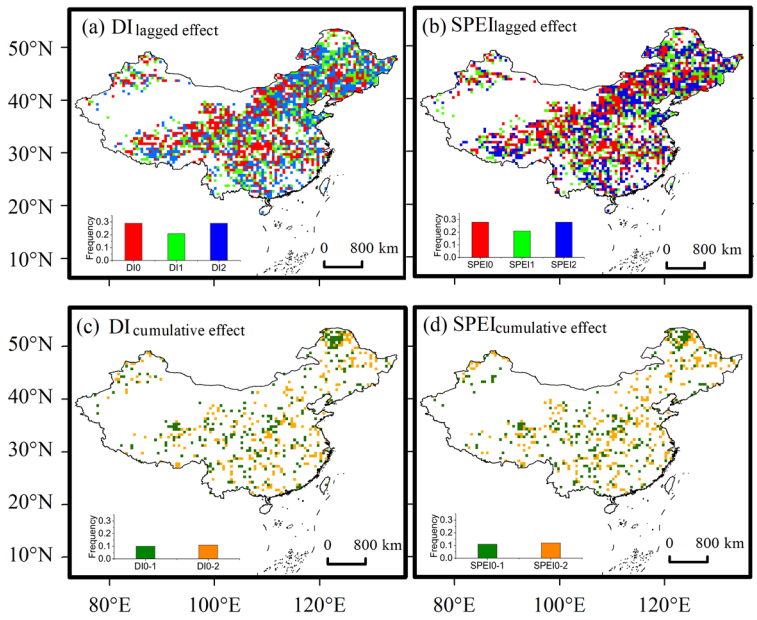

Figure 8. The lagged effect (**a**,**b**) and cumulative effect (**c**,**d**) of DI/SPEI on POG determined by the absolute maximum correlation coefficient.

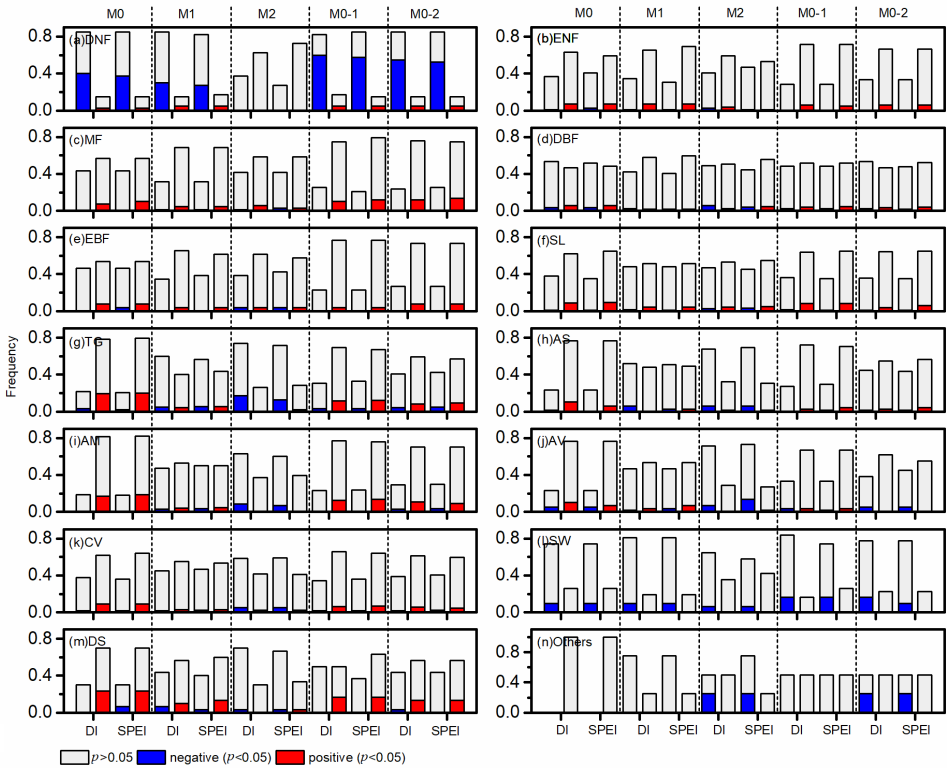

Figure 9. Percentage of negative and positive correlations between POG and DI/SPEI in different periods for divergent biomes. M0, M1, M2, M0-1, and M0-2 are the same as Figure 7.

We also investigated the changes in $R_{POG\_drought\ index}$ with elevation for different biomes. The significant correlations among DNF, MF, TG, and AM are shown in Figure 10, and those for all biomes can be found in Figure S2. Regarding DNF, $R_{POG\_drought\ index}$ ranged from −0.6 at lower elevations to 0.4 at higher elevations up to 3000 m, indicating an intricate effect of available water on POG at different elevations. In terms of MF, TG, and AM, POG was not affected by drought in lower-lying areas, as indicated by an $R_{POG\_drought\ index}$ value close to 0. However, with increasing elevation, $R_{POG\_drought\ index}$ increased significantly in MF and MG, while it decreased significantly in AM ($p < 0.01$).

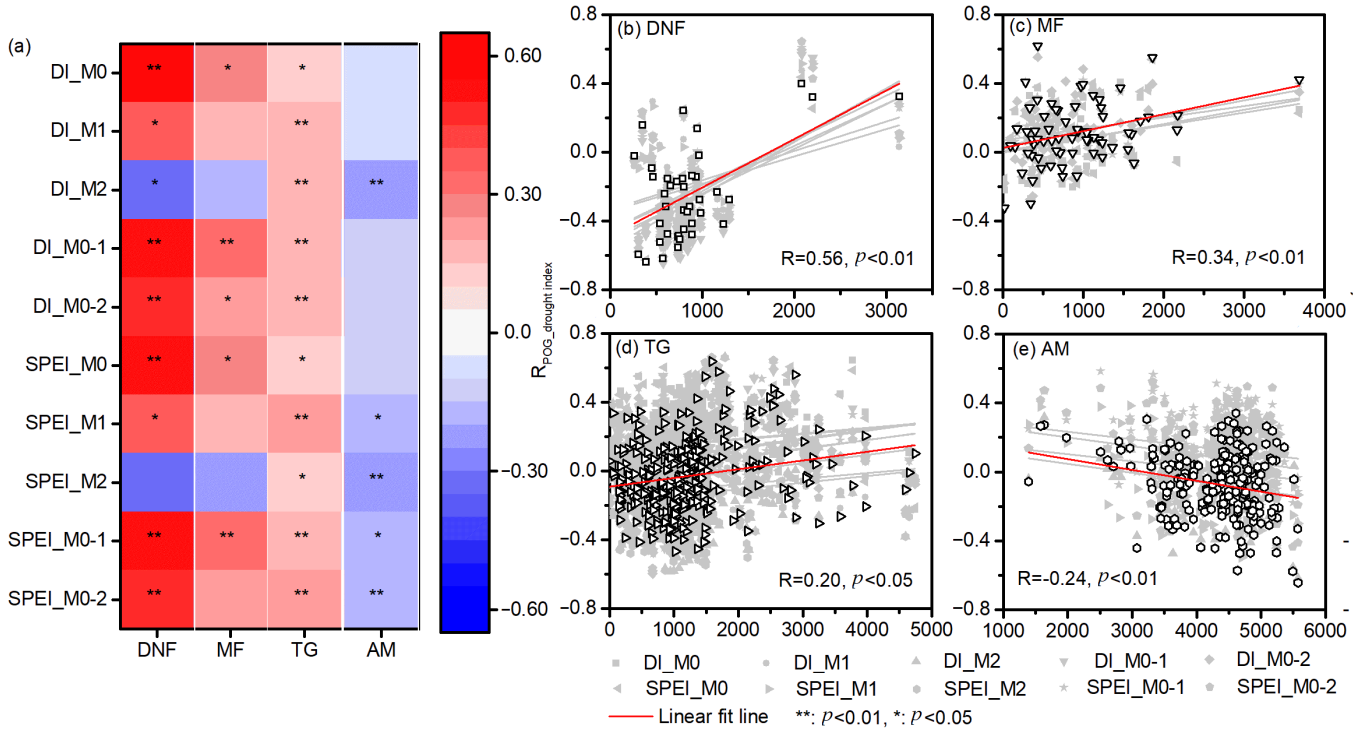

Figure 10. Pearson's correlation coefficients between $R_{POG\_drought\ index}$ and elevation for biomes that showed significant changes in $R_{POG\_drought\ index}$ along the elevation gradient (**a**). $R_{POG\_drought\ index}$ represents Pearson's correlation coefficient between POG and SPEI/DI. The symbols in bold show the months in which $R_{POG\_drought\ index}$ has the largest absolute correlation coefficient with elevation for DNF (**b**), MF (**c**), TG (**d**), and AM (**e**).

4. Discussion

4.1. Patterns of Drought and the Drivers

Drought is a widely occurring climatic event and, in synergy with warming, can have various effects on vegetation phenology [29,42]. Increased aridity over the past decades has been revealed by historical records of precipitation, streamflow, and drought indices across the world [28]. In this study, we also found an overall trend towards aridity in most areas of China over the past three decades based on two drought indices (Figure 4). The areas with the most significant drying trend were mainly located around the Tarim Basin in northwest China and the Yunnan-Guizhou Plateau in southwest China, which is consistent with other studies [32].

According to the formula of the drought index, the trend towards drought is generally attributed to reduced precipitation and increased evapotranspiration [31]. However, we noticed that the annual precipitation even increased during the study period in some areas with a drying trend. This may be due to the fact that increased evapotranspiration makes a larger contribution than precipitation changes to determining the drying trend [43]. Considering that the total amount of water loss is related to various climate factors, we further analyzed the correlations among POG and four potential climate factors, i.e., temperature,

precipitation, radiation, and wind speed in M0-1, through a partial correlation analysis to estimate the most important factor affecting the changes in drought. Compared with other factors, a closer correlation was found between wind speed and POG in ca. 15%~35% of the areas for different biomes (Figure S3). Increased winds would enhance evapotranspiration and reduce water availability [44], thus leading to a trend towards aridity, that is, a decrease in the drought index.

4.2. Response of POG to Drought in Different Periods

Our results highlighted a heterogeneous influence of droughts on the POG for different periods. In general, a spring drought that mainly occurred in the second month before the multiyear average POG (M2) would postpone POG, especially in northern China, while a summer drought that appeared in the current month of the multiyear average POG (M0) would lead to an advance in POG. It reflects the divergent response mechanism of plant growth to moisture conditions. On the one hand, spring drought may retard plant growth and lead to a delay in spring phenology [45,46]. The start of peak plant activity will also arrive later in response to the later start of spring phenology [14,19]. On the other hand, plants have to close the stomata in their leaves in order to minimize evapotranspiration during summer droughts [47], which may indirectly reduce the carbon uptake and photosynthetic capacity of plants. Thus, the early emergence of POG, i.e., the timing of the maximum capacity of photosynthesis rate, will allow plants to avoid potentially unbearable drought risk in summer [21,48]. Similarly, good moisture conditions in summer are likely to lengthen the period that is suitable for plant growth, so that plants reach their maximum capacity of photosynthesis later.

4.3. Response of POG to Drought in Different Biomes

Our research indicated that the response of POG to drought conditions varies significantly across biomes. In most biomes, POG was positively correlated with the pre-season DI/SPEI, suggesting that POG occurred earlier under drier conditions. This can be explained by the fact that drought typically results from insufficient rainfall to replenish soil moisture adequately, leading to reduced soil moisture that subsequently hinders plant growth by decreasing the maximum photosynthetic rate, thereby precipitating an earlier onset of phenology [49,50]. However, in DNF, TG, and SW, an inverse correlation predominated, indicating a delayed POG in response to drought. This might be because drought is often accompanied by reduced cloud cover and increased radiation [51], enhancing radiation that increases photosynthetic activity in vegetation and consequently delaying the POG [52], as observed in DNF and TG.

Previous studies also confirmed significant variability in the POG response to drought among different biomes, which was influenced by a combination of factors including precipitation, soil moisture, cloud cover, and radiation. For instance, in most biomes of the Northern Hemisphere, precipitation positively correlates with POG, implying an earlier onset under drier conditions [53]. In AS and AM of China, soil moisture was positively correlated with POG, whereas it was negatively correlated with TG [18]. In TG in the Mongolian Plateau, POG was negatively correlated with the SPEI from two months prior to the season [54]. These findings were largely consistent with our research. Additionally, the impact intensity of drought varied across different biomes. Grasslands, for instance, exhibited a relatively greater response to drought compared with other biomes such as forests [52]. Typically, grasslands have shallower root systems, making them more sensitive to precipitation and less able to access deep water supplies [55].

4.4. Response of POG to Drought along the Moisture Gradient

It is worth noting that POG responds divergently in different biomes along the moisture gradient. In relatively dry regions, the summer drought is related to an earlier POG. However, the negative effects of drought weaken with increasing background humidity (Figure 9). In relatively wet regions (e.g., DNF, SW, DBF), where plants can always obtain

enough water for growth, a summer drought may inversely diminish the photosynthetic rate of plants, therefore leading to a late arrival of the peak photosynthetic activity.

4.5. Response of POG to Drought with Changes in Elevation

In addition, a remarkable heterogeneity in the phenological response to droughts was found with changes in elevation (Figure 10). It is believed that this pattern of the POG–drought relationship is restricted by various climate factors [56]. For example, POG is closely correlated with radiation in more than 60% of the DNF region (Figure S3). Plants at higher elevations receive sufficient radiation to improve the efficiency of photosynthesis as the available humidity increases, which can lead to a delay in POG and a closer relationship between the drought index and POG. On the contrary, the radiation is relatively weak at lower elevations, and an increase in humidity would further reduce radiation and weaken photosynthesis [19]. As a result, the increase in humidity under radiation restriction no longer leads to an increase in photosynthetic efficiency, and the relationship between POG and the drought index is much lower.

4.6. Uncertainties

The responses of vegetation to climate change exhibit relative similarities within the same vegetation type (or land covers), making the use of biomes a common approach for comparative analysis. This method is prevalent in previous ecological and phenological studies [57,58]. However, it is important to recognize that when dealing with large regional scales, variations in the same type of vegetation are inevitable. These differences can be attributed to vegetation adaption to local climate conditions. For example, vegetation in arid regions may exhibit lower vulnerability and sensitivity to hot drought than that in humid regions. Nevertheless, it is worth noting that the variance in a single biome is usually much smaller than the difference between distinct biomes. In addition, it must be acknowledged that vegetation phenology is affected by human activities, particularly in biomes such as cultivated vegetation (CV). At present, the task of quantifying these impacts on a global scale remains a considerable challenge because of the complexity of various human control measures. In this study, we only examined the patterns of drought and how vegetation phenology responds to changes in drought conditions on a relatively broad scale. We acknowledge that our findings may not be sufficient to provide comprehensive information in climatically heterogeneous regions, which may require more detailed investigations at local scales for each region in future studies.

5. Conclusions

Based on two drought indices and NDVI series from the GIMMS3g dataset, we analyzed the temporal–spatial pattern of drought events and the peak of growing season across different biomes in China. We then investigated how drought influenced POG in different periods of the early season using correlation analysis. Despite significant spatial heterogeneity, increased aridity and a trend towards earlier POG were observed in most areas. The influence of drought on POG varied across different periods and biomes. Generally, drought occurring near POG results in an earlier onset of POG. On the contrary, a drought that occurs 2 months before POG will lead to a delay in POG. Regarding different biomes, a summer drought led to an earlier POG in relatively dry biomes but resulted in a late arrival of peak photosynthetic activity in relatively wet biomes. We also observed a one- or two-month lagged effect of drought on POG in almost half of the areas, and a two- or three-month cumulative effect in the northern regions above 50° N. Our findings may contribute to a better understanding of how climate change affects vegetation growth and photosynthetic activity, as well as carbon assimilation in terrestrial ecosystems.

Supplementary Materials: The following supporting information can be downloaded at: https://www.mdpi.com/article/10.3390/f15061027/s1, Figure S1. The Pearson's correlation coefficients and p-values between POG and DI/SPEI in different periods; Figure S2. The Pearson's correlation

coefficient between RPOG_drought index and elevation for different biomes; Figure S3. Partial correlation coefficient and significance between POG and (a,b) temperature, (c,d) total precipitation, (e,f) total radiation, (g,h) wind speed, and most related factors (i) across China, and (j) in different vegetation regions.

Author Contributions: Resources, X.W.; Writing—original draft, Z.T.; Writing—review & editing, Y.W.; Supervision, J.D. All authors have read and agreed to the published version of the manuscript.

Funding: This research was supported by the National Key Research and Development Program of China (grant no. 2023YFF1303804) and the National Natural Science Foundation of China (grant no. 42271062).

Data Availability Statement: The data presented in this study are available on request from the corresponding author. The data are not publicly available due to privacy.

Conflicts of Interest: The authors declare no conflict of interest.

References

1. Primack, R.B.; Laube, J.; Gallinat, A.S.; Menzel, A. From observations to experiments in phenology re-search, investigating climate change impacts on trees and shrubs using dormant twigs. *Ann. Bot.* **2015**, *116*, 889–897. [CrossRef] [PubMed]
2. Richardson, A.D.; Keenan, T.F.; Migliavacca, M.; Ryu, Y.; Sonnentag, O.; Toomey, M. Climate change, phenology, and phenological control of vegetation feedbacks to the climate system. *Agric. For. Meteorol.* **2013**, *169*, 156–173. [CrossRef]
3. Sun, Q.; Li, B.; Zhou, G.; Jiang, Y.; Yuan, Y. Delayed autumn leaf senescence date prolongs the growing season length of herbaceous plants on the Qinghai-Tibetan Plateau. *Agric. For. Meteorol.* **2020**, *284*, 107896. [CrossRef]
4. Visser, M.E. Phenology, Interactions of climate change and species. *Nature* **2016**, *535*, 236–237. [CrossRef] [PubMed]
5. Keenan, T.F.; Gray, J.; Friedl, M.A.; Toomey, M.; Bohrer, G.; Hollinger, D.Y.; Munger, J.W.; O'Keefe, J.; Schmid, H.P.; Wing, I.S.; et al. Net carbon uptake has increased through warming-induced changes in temperate forest phenology. *Nat. Clim. Chang.* **2014**, *4*, 598–604. [CrossRef]
6. Lian, X.; Piao, S.; Li, L.Z.X.; Li, Y.; Huntingford, C.; Ciais, P.; Cescatti, A.; Janssens, I.A.; Peñuelas, J.; Buermann, W.; et al. Summer soil drying exacerbated by earlier spring greening of northern vegetation. *Sci. Adv.* **2020**, *6*, eaax0255. [CrossRef]
7. Meng, F.; Zhang, L.; Zhang, Z.; Jiang, L.; Wang, Y.; Duan, J.; Wang, Q.; Li, B.; Liu, P.; Hong, H.; et al. Enhanced spring temperature sensitivity of carbon emission links to earlier phenology. *Sci. Total Environ.* **2020**, *745*, 140999. [CrossRef] [PubMed]
8. Murthy, K.; Bagchi, S. Spatial patterns of long-term vegetation greening and browning are con-sistent across multiple scales, Implications for monitoring land degradation. *Land Degrad. Dev.* **2018**, *29*, 2485–2495. [CrossRef]
9. Buermann, W.; Forkel, M.; O'Sullivan, M.; Sitch, S.; Friedlingstein, P.; Haverd, V.; Jain, A.K.; Kato, E.; Kautz, M.; Lienert, S.; et al. Widespread seasonal compensation effects of spring warming on northern plant productivity. *Nature* **2018**, *562*, 110–114. [CrossRef] [PubMed]
10. Peng, D.; Wang, Y.; Xian, G.; Huete, A.R.; Huang, W.; Shen, M.; Wang, F.; Yu, L.; Liu, L.; Xie, Q.; et al. Investigation of land surface phenology detections in shrub-lands using multiple scale satellite data. *Remote Sens. Environ.* **2020**, *252*, 112133. [CrossRef]
11. Wu, C.; Hou, X.; Peng, D.; Gonsamo, A.; Xu, S. Land surface phenology of China's temperate ecosystems over 1999–2013, Spatial-temporal patterns, interaction effects, covariation with climate and implications for productivity. *Agric. For. Meteorol.* **2016**, *216*, 177–187. [CrossRef]
12. Yun, J.; Jeong, S.-J.; Ho, C.-H.; Park, C.-E.; Park, H.; Kim, J. Influence of winter precipitation on spring phenology in boreal forests. *Glob. Chang. Biol.* **2018**, *24*, 5176–5187. [CrossRef] [PubMed]
13. Ge, Z.; Huang, J.; Wang, X.; Zhao, Y.; Tang, X.; Zhou, Y.; Lai, P.; Hao, B.; Ma, M. Using remote sensing to identify the peak of the growing sea-son at globally-distributed flux sites, A comparison of models, sensors, and biomes. *Agric. For. Meteorol.* **2021**, *307*, 108489. [CrossRef]
14. Gonsamo, A.; Chen, J.M.; Ooi, Y.W. Peak season plant activity shift towards spring is reflected by increasing carbon uptake by extratropical ecosystems. *Glob. Chang. Biol.* **2018**, *24*, 2117–2128. [CrossRef] [PubMed]
15. Hilton, T.W.; Whelan, M.E.; Zumkehr, A.; Kulkarni, S.; Berry, J.A.; Baker, I.T.; Montzka, S.A.; Sweeney, C.; Miller, B.R.; Elliott Campbell, J. Peak growing season gross uptake of carbon in North America is largest in the Midwest USA. *Nat. Clim. Chang.* **2017**, *7*, 450–454. [CrossRef]
16. Park, T.; Ganguly, S.; Tømmervik, H.; Euskirchen, E.S.; Høgda, K.-A.; Karlsen, S.R.; Brovkin, V.; Nemani, R.R.; Myneni, R.B. Changes in growing season duration and productivity of northern vegetation inferred from long-term remote sensing data. *Environ. Res. Lett.* **2016**, *11*, 084001. [CrossRef]
17. Yang, F.; Liu, C.; Chen, Q.; Lai, J.; Liu, T. Earlier spring-summer phenology and higher photosynthetic peak altered the seasonal patterns of vegetation productivity in alpine ecosystems. *Remote Sens.* **2024**, *16*, 1580. [CrossRef]
18. Yang, J.; Dong, J.; Xiao, X.; Dai, J.; Wu, C.; Xia, J.; Zhao, G.; Zhao, M.; Li, Z.; Zhang, Y.; et al. Divergent shifts in peak photosynthesis timing of temper-ate and alpine grasslands in China. *Remote Sens. Environ.* **2019**, *233*, 111395. [CrossRef]
19. Wang, X.Y.; Wu, C.Y. Estimating the peak of growing season (POS) of China's terrestrial eco-systems. *Agric. For. Meteorol.* **2019**, *278*, 107639. [CrossRef]

20. Zeng, Z.; Piao, S.; Li, L.Z.X.; Zhou, L.; Ciais, P.; Wang, T.; Li, Y.; Lian, X.; Wood, E.F.; Friedlingstein, P.; et al. Climate mitigation from vegetation biophysical feedbacks during the past three decades. *Nat. Clim. Chang.* **2017**, *7*, 432–436. [CrossRef]
21. Xu, C.; Liu, H.; Williams, A.P.; Yin, Y.; Wu, X. Trends toward an earlier peak of the growing season in Northern Hemisphere mid-latitudes. *Glob. Chang. Biol.* **2016**, *22*, 2852–2860. [CrossRef] [PubMed]
22. Cleland, E.E.; Chuine, I.; Menzel, A.; Mooney, H.A.; Schwartz, M.D. Shifting plant phenology in response to global change. *Trends Ecol. Evol.* **2007**, *22*, 357–365. [CrossRef] [PubMed]
23. Fu, Y.H.; Zhao, H.; Piao, S.; Peaucelle, M.; Peng, S.; Zhou, G.; Ciais, P.; Huang, M.; Menzel, A.; Peñuelas, J.; et al. Declining global warming effects on the phenology of spring leaf unfolding. *Nature* **2015**, *526*, 104–107. [CrossRef] [PubMed]
24. Maseyk, K.S.; Lin, T.; Rotenberg, E.; Grünzweig, J.M.; Schwartz, A.; Yakir, D. Physiology-phenology interactions in a productive semi-arid pine forest. *New Phytol.* **2008**, *178*, 603–616. [CrossRef] [PubMed]
25. Schimel, D.S. Drylands in the Earth System. *Science* **2010**, *327*, 418–419. [CrossRef] [PubMed]
26. Esch, E.H.; Lipson, D.A.; Cleland, E.E. Invasion and drought alter phenological sensitivity and synergistically lower ecosystem production. *Ecology* **2019**, *100*, e02802. [CrossRef] [PubMed]
27. Allen, C.D.; Breshears, D.D.; McDowell, N.G. On underestimation of global vulnerability to tree mortality and forest die-off from hotter drought in the Anthropocene. *Ecosphere* **2015**, *6*, 1–55. [CrossRef]
28. Dai, A. Increasing drought under global warming in observations and models. *Nat. Clim. Chang.* **2013**, *3*, 52–58. [CrossRef]
29. Deng, H.; Yin, Y.; Wu, S.; Xu, X. Contrasting drought impacts on the start of phenological growing season in Northern China during 1982–2015. *Int. J. Climatol.* **2020**, *40*, 3330–3347. [CrossRef]
30. Li, B.; Su, H.; Chen, F.; Wu, J.; Qi, J. The changing characteristics of drought in China from 1982 to 2005. *Nat. Hazards* **2013**, *68*, 723–743. [CrossRef]
31. Sheffield, J.; Wood, E.F.; Roderick, M.L. Little change in global drought over the past 60 years. *Nature* **2012**, *491*, 435–438. [CrossRef] [PubMed]
32. Zeng, Z.; Wu, W.; Li, Y.; Zhou, Y.; Zhang, Z.; Zhang, S.; Guo, Y.; Huang, H.; Li, Z. Spatiotemporal Variations in Drought and Wetness from 1965 to 2017 in China. *Water* **2020**, *12*, 2097. [CrossRef]
33. Groisman, P.; Bulygina, O.; Henebry, G.; Speranskaya, N.; Shiklomanov, A.; Chen, Y.; Tchebakova, N.; Parfenova, E.; Tilinina, N.; Zolina, O.; et al. Dryland belt of Northern Eurasia, contemporary environmental changes and their consequences. *Environ. Res. Lett.* **2018**, *13*, 115008. [CrossRef]
34. Pinzon, J.E.; Tucker, C.J. A Non-Stationary 1981–2012 AVHRR NDVI3g Time Series. *Remote Sens.* **2014**, *6*, 6929–6960. [CrossRef]
35. Tao, Z.; Wang, H.; Liu, Y.; Xu, Y.; Dai, J. Phenological response of different vegetation types to temperature and precipitation variations in northern China during 1982–2012. *Int. J. Remote Sens.* **2017**, *38*, 3236–3252. [CrossRef]
36. Yang, K.; He, J. China meteorological forcing dataset (1979–2015). In *A Big Earth Data Platform for Three Poles*; National Tibetan Plateau Data Center: Beijing, China, 2016. Available online: https://poles.tpdc.ac.cn/zh-hans/data/7a35329c-c53f-4267-aa07-e0037d913a21/ (accessed on 7 May 2024). [CrossRef]
37. Cong, N.; Shen, M.; Piao, S.; Chen, X.; An, S.; Yang, W.; Fu, Y.H.; Meng, F.; Wang, T. Little change in heat requirement for vegetation green-up on the Tibetan Plateau over the warming period of 1998–2012. *Agric. For. Meteorol.* **2017**, *232*, 650–658. [CrossRef]
38. Vicente-Serrano, S.M.; Beguería, S.; López-Moreno, J.I. A Multiscalar Drought Index Sensitive to Global Warming, The Standardized Precipitation Evapotranspiration Index. *J. Clim.* **2010**, *23*, 1696–1718. [CrossRef]
39. Jiang, D.; Hao, M.; Fu, J.; Zhuang, D.; Huang, Y. Spatial-temporal variation of marginal land suitable for energy plants from 1990 to 2010 in China. *Sci. Rep.* **2014**, *4*, 5816. [CrossRef] [PubMed]
40. Ohlson, J.A.; Kim, S. Linear valuation without OLS, the Theil-Sen estimation approach. *Rev. Account. Stud.* **2015**, *20*, 395–435. [CrossRef]
41. Peng, J.; Wu, C.; Zhang, X.; Wang, X.; Gonsamo, A. Satellite detection of cumulative and lagged effects of drought on autumn leaf senescence over the Northern Hemisphere. *Glob. Chang. Biol.* **2019**, *25*, 2174–2188. [CrossRef] [PubMed]
42. Jiao, W.; Wang, L.; Smith, W.K.; Chang, Q.; Wang, H.; D'Odorico, P. Observed increasing water constraint on vegetation growth over the last three decades. *Nat. Commun.* **2021**, *12*, 3777. [CrossRef]
43. Sun, S.; Chen, H.; Ju, W.; Wang, G.; Sun, G.; Huang, J.; Ma, H.; Gao, C.; Hua, W.; Yan, G. On the coupling between precipitation and potential evapo-transpiration, contributions to decadal drought anomalies in the Southwest China. *Clim. Dyn.* **2017**, *48*, 3779–3797. [CrossRef]
44. Wu, C.; Wang, J.; Ciais, P.; Peñuelas, J.; Zhang, X.; Sonnentag, O.; Tian, F.; Wang, X.; Wang, H.; Liu, R.; et al. Widespread decline in winds delayed autumn foliar senescence over high latitudes. *Proc. Natl. Acad. Sci. USA* **2021**, *118*, e2015821118. [CrossRef] [PubMed]
45. Liu, Q.; Fu, Y.H.; Zeng, Z.; Huang, M.; Li, X.; Piao, S. Temperature, precipitation, and insolation effects on autumn vegetation phenology in temperate China. *Glob. Chang. Biol.* **2016**, *22*, 644–655. [CrossRef] [PubMed]
46. Tao, Z.; Huang, W.; Wang, H. Soil moisture outweighs temperature for triggering the green-up date in temperate grasslands. *Theor. Appl. Climatol.* **2020**, *140*, 1093–1105. [CrossRef]
47. Arend, M.; Brem, A.; Kuster, T.M.; Günthardt-Goerg, M.S. Seasonal photosynthetic responses of European oaks to drought and elevated daytime temperature. *Plant Biol.* **2013**, *15*, 169–176. [CrossRef] [PubMed]

48. Montserrat-Martí, G.; Camarero, J.J.; Palacio, S.; Pérez-Rontomé, C.; Milla, R.; Albuixech, J.; Maestro, M. Summer-drought constrains the phenology and growth of two coexisting Mediterranean oaks with contrasting leaf habit, implications for their persistence and reproduction. *Trees* **2009**, *23*, 787–799. [CrossRef]
49. Hufkens, K.; Keenan, T.F.; Flanagan, L.B.; Scott, R.L.; Bernacchi, C.J.; Joo, E.; Brunsell, N.A.; Verfaillie, J.; Richardson, A.D. Productivity of North American grasslands is increased under future climate scenarios de-spite rising aridity. *Nat. Clim. Chang.* **2016**, *6*, 710–714. [CrossRef]
50. Liu, D.; Li, Y.; Wang, T.; Peylin, P.; MacBean, N.; Ciais, P.; Jia, G.; Ma, M.; Ma, Y.; Shen, M.; et al. Contrasting responses of grassland water and carbon exchanges to climate change between Tibetan Plateau and Inner Mongolia. *Agric. For. Meteorol.* **2018**, *249*, 163–175. [CrossRef]
51. Liu, Y.; Wu, C.; Wang, X.; Jassal, R.S.; Gonsamo, A. Impacts of global change on peak vegeta-tion growth and its timing in terrestrial ecosystems of the continental US. *Glob. Planet. Chang.* **2021**, *207*, 103657. [CrossRef]
52. Li, G.; Wu, C.; Chen, Y.; Huang, C.; Zhao, Y.; Wang, Y.; Ma, M.; Ding, Z.; Yu, P.; Tang, X. Increasing temperature regu-lates the advance of peak photosynthesis timing in the boreal ecosystem. *Sci. Total Environ.* **2023**, *882*, 163587. [CrossRef] [PubMed]
53. Huang, Z.; Zhou, L.; Chi, Y. Spring phenology rather than climate dominates the trends in peak of growing season in the Northern Hemisphere. *Glob. Chang. Biol.* **2023**, *29*, 4543–4555. [CrossRef] [PubMed]
54. Bai, Y.; Li, S. Growth peak of vegetation and its response to drought on the Mongolian Plateau. *Ecol. Indic.* **2022**, *141*, 109150. [CrossRef]
55. Zeng, X.; Hu, Z.; Chen, A.; Yuan, W.; Hou, G.; Han, D.; Liang, M.; Di, K.; Cao, R.; Luo, D. The global decline in the sen-sitivity of vegetation productivity to precipitation from 2001 to 2018. *Glob. Chang. Biol.* **2022**, *28*, 6823–6833. [CrossRef] [PubMed]
56. Bradley, A.V.; Gerard, F.F.; Barbier, N.; Weedon, G.P.; Anderson, L.O.; Huntingford, C.; AragÃO, L.E.O.C.; Zelazowski, P.; Arai, E. Relationships between phenology, radiation and precip-itation in the Amazon region. *Glob. Chang. Biol.* **2011**, *17*, 2245–2260. [CrossRef]
57. Wu, C.; Peng, J.; Ciais, P.; Peñuelas, J.; Wang, H.; Beguería, S.; Andrew Black, T.; Jassal, R.S.; Zhang, X.; Yuan, W.; et al. Increased drought effects on the phenology of autumn leaf senes-cence. *Nat. Clim. Chang.* **2022**, *12*, 943–949. [CrossRef]
58. Gampe, D.; Zscheischler, J.; Reichstein, M.; O'Sullivan, M.; Smith, W.K.; Sitch, S.; Buermann, W. Increasing impact of warm droughts on northern ecosystem productivity over recent decades. *Nat. Clim. Chang.* **2021**, *11*, 772–779. [CrossRef]